



# Experimental and numerical investigation of the promoting effect of a cetane booster in a low-octane gasoline fuel in a rapid compression machine: A study of 2-ethylhexyl nitrate

Minh Duy Le, Mickaël Matrat, Arij Ben Amara, Fabrice Foucher, Bruno Moreau, Yi Yu, Pierre-Alexandre Glaude

## ► To cite this version:

Minh Duy Le, Mickaël Matrat, Arij Ben Amara, Fabrice Foucher, Bruno Moreau, et al.. Experimental and numerical investigation of the promoting effect of a cetane booster in a low-octane gasoline fuel in a rapid compression machine: A study of 2-ethylhexyl nitrate. *Combustion and Flame*, 2020, 222, pp.36-47. 10.1016/j.combustflame.2020.08.024 . hal-02931250

HAL Id: hal-02931250

<https://hal.science/hal-02931250>

Submitted on 16 Dec 2020

**HAL** is a multi-disciplinary open access archive for the deposit and dissemination of scientific research documents, whether they are published or not. The documents may come from teaching and research institutions in France or abroad, or from public or private research centers.

L'archive ouverte pluridisciplinaire **HAL**, est destinée au dépôt et à la diffusion de documents scientifiques de niveau recherche, publiés ou non, émanant des établissements d'enseignement et de recherche français ou étrangers, des laboratoires publics ou privés.

**Experimental and Numerical Investigation of the Promoting Effect of a Cetane Booster in a Low-Octane Gasoline Fuel in a Rapid Compression Machine: a Study of 2-Ethylhexyl Nitrate**

Minh Duy Le<sup>a,c</sup>, Mickaël Matrat<sup>a,1\*</sup>, Arij Ben Amara<sup>a</sup>, Fabrice Foucher<sup>b</sup>, Bruno Moreau<sup>b</sup>, Yi Yu<sup>b</sup>, Pierre-Alexandre Glaude<sup>c</sup>

<sup>a</sup>*IFP Energies Nouvelles, 1 et 4, avenue de Bois-Préau, 92852 Rueil-Malmaison Cedex, France*

<sup>b</sup>*Univ. Orléans, INSA-CVL, PRISME, EA 4229, F45072, Orléans, France*

<sup>c</sup>*LRGP, CNRS-Université de Lorraine, 1, rue Grandville, 54000 Nancy, France*

---

\* Corresponding author: [mickael.marat@ifpen.fr](mailto:mickael.marat@ifpen.fr); Tel: +33 1 47 5251 10

## Abstract

Modern societies require cleaner and more efficient internal combustion engines. Low-temperature combustion (LTC) has been proved to be a good step toward this goal. This study aims at investigating the promoting effect of a cetane booster additive named 2-ethylhexyl nitrate (EHN) on the reactivity of a low-octane gasoline at LTC-relevant conditions. Rapid compression machine experiments were conducted at 10 bar, from 675 to 960 K for stoichiometric mixtures. The neat fuel was a mixture of toluene and *n*-heptane whose research octane number is 84. The doping levels of the additive were set at 0.1 and 1% molar basis. At the experimental conditions, it is found that EHN provides a promoting effect on the surrogate reactivity over all the whole temperature range. This effect increases with EHN doping levels. The negative temperature coefficient (NTC) behavior of the surrogate fuel is mitigated by the presence of the additive. The EHN reactivity promoting effect is lowest around 710 K and then increases with temperature. Under some conditions, heat releases are observed during the compression process. The chemical reactivity of the fuel gas mixture during the piston movement has to be considered to get reliable simulations. Kinetic modeling works show a good agreement with experiments. The model of this study reproduces properly the EHN promoting effect over the whole range of investigated temperatures and doping levels. Numerical analyses were conducted. EHN can totally decompose during the compression process resulting in heat releases. EHN is less effective at low T<sub>c</sub> (< 800 K) at lean condition than at stoichiometric condition. It is found that the EHN effect links to the OH radical formation and the NO<sub>2</sub>-NO loop. The reactions between NO and *n*-heptyl peroxy radicals are found to be the main reason for the EHN effect in NTC region of the surrogate fuel oxidation.

Key words: Fuel additive; 2-ethylhexyl nitrate; nitrogen chemistry; rapid compression machine; kinetic modeling; low temperature combustion

## 1. Introduction

Global warming urges researchers to improve internal combustion (IC) engines, which are dominantly used in the automotive industry. IC engines are required to operate more efficiently while reducing pollutant and greenhouse gas emissions simultaneously. Low temperature combustion (LTC) [1] has proved to be a promising method to achieve a great step in engine development. LTC is studied in diverse forms such as homogenous charge compression ignition (HCCI) [2] gasoline compression ignition (GCI) [3], reactivity controlled compression ignition (RCCI) [4], and spark assisted compression ignition (SACI) [5]. All these techniques expect an in-depth comprehension of fuel chemical reactivity since the fuel itself controls the auto-ignition and remains a key parameter for combustion emissions.

Autoignition chemistry of fuels at engine-relevant conditions has been investigated fundamentally in various equipment comprising shock tube (ST) and rapid compression machine (RCM). While ST is used to capture fuel reactivity at high temperature ( $T > 900$  K) [6], RCM helps to characterize fuel autoignition at a lower temperature range ( $T < 900$  K) [7]. Thus, RCM is a suitable technique to investigate LTC. For an RCM test, the fuel gas mixture is compressed to the desired thermodynamic conditions thanks to the piston movement. Once the piston stops, the ignition occurs in a constant volume chamber. Mohamed et al. [8] have noticed that gas reactions could occur before the end of piston movement by investigating the autoignition of *n*-pentane and *n*-heptane. Any starting reactivity before the compression ends should be considered to get a reliable simulated ignition delay

time (IDT) of high reactivity fuels as described by Curran et al. [9].

To control fuel reactivity, additives have been employed for a long time. Tetraethyl lead was largely used as an octane booster to prevent knocking in spark-ignition (SI) [10] while numerous nitrates and peroxide compounds can enhance efficiently cetane number of diesel fuels [11,12]. Using additive is an efficient method to get the desired combustion timing in LTC engines [1]. 2-Ethylhexyl nitrate (EHN) is a commercial additive that boosts diesel fuel reactivity. This molecule contains a weak N-O bond ( $E_{\text{RO-NO}_2} \approx 40.7 \text{ kcal/mol}$ ) [13], which can break rapidly into radicals and then enhance fuel reactivity. This additive has been investigated in engines operating at LTC conditions [14,15]. Despite the wide use of EHN, the fundamental studies of EHN promoting effect are still scarce. Hartmann et al. [16] performed a ST study of a high reactivity fuel (*n*-heptane having research octane number (RON) of zero) doped with EHN at high pressure (40 bar) from 690 to 1275 K. The EHN promoting effect was also examined in very low reactivity fuels (RON > 90) by Cadman et al. [17] and Goldsborough et al. [18]. These studies show a complex behavior of EHN promoting effect depending on fuels, air/fuel mixture and thermodynamic conditions. The EHN effect on a low-octane gasoline fuel in a state-of-the-art RCM of the University of Orleans has been recently performed [19] at lean conditions. The simulation results obtained by adopting a frozen chemistry assumption during the compression process agree reasonably well with the experimental results. However, this cannot ensure a similar observation if the compressed gas mixture is more reactive. That would be the case for example with stoichiometric mixtures where ignition delays would be shorter for the base fuel.

The motivation of this study is: (1) to provide a set of experimental data about the EHN promoting effect on a moderate reactivity fuel, which is a low-octane gasoline fuel at conditions relevant to LTC combustion; and (2) to present a validated kinetic model of EHN, involving an up-to-date mechanism for hydrocarbon and nitrogen containing species. This is essential for exploring the additive effect beyond the experimental limits in order to discuss the EHN chemical effect. The IDT measurements were performed in an RCM. Modeling investigations were conducted to understand EHN action during compression process. This aspect has been little examined in previous studies. The main reactions representing EHN effect are further discussed in this paper.

## 2. Experimental Methods

In this study, IDT measurements were performed in the single-piston RCM of the University of Orleans. The compression technique and the crevices geometry of this RCM were built based on the RCM developed at the Argonne National Laboratory [20]. This RCM contains a creviced piston to avoid the vortex formation and to ensure the post-combustion charge homogeneity. The use of a creviced piston, which is largely employed in previous experimental works [21–23], helps to study the hydrocarbon autoignition chemistry limiting physical effects. Further details of the RCM of the University of Orleans can be accessed elsewhere [19,24], only a brief description of this machine is presented here. The stroke and the bore of the RCM have a length of 300 mm and 50 mm respectively. In this study, the compression ratio varies from 8.9 to 20.7. The hydraulic technique is used to lock the piston at the top dead center after the compression process which lasts about 33 ms.

The in-cylinder pressure history was recorded by an AVL QH32C piezoresistive transducer while the intake pressure was followed by a Keller PAA-33X/80794. The gas preparation reservoir temperature and piston initial temperature were measured by K thermocouples. The gas mass flow rates were regulated by Bronkhorst Cori-flow M13. The errors of measurement of in-cylinder pressure, intake pressure, intake temperatures, and mass flow rate are  $\pm 1\%$ ,  $\pm 1$  mbar,  $\pm 2$  K and  $\pm 1\%$  respectively.

In this work, the high purity liquid fuels including toluene (99.8%), *n*-heptane (99%) and EHN (97%) from Sigma-Aldrich were employed. The surrogate fuel is a mixture of toluene (65% vol.) and *n*-heptane (35% vol.) having a research octane number (RON) of 84 which was given in the work of Herzler et al. [25]. This surrogate fuel helps to understand the EHN effect on some specific phenomena of ignitions, which are two-stage ignitions and the negative temperature coefficient (NTC). The doped fuels were prepared gravimetrically. EHN doping levels were 0.1 and 1% on molar basis with a relative uncertainty below 1%. To obtain the stoichiometric proportion, the gaseous fuel was premixed with the synthetic air (21% mol. O<sub>2</sub>, 79% mol. N<sub>2</sub>) from Air Liquide in a reservoir at 3 bar. Before the mixtures preparation, the reservoir was flushed with air and then pumped out to vacuum (< 1 mbar), which ensured no compound accumulated in the reservoir. The liquid fuels doped with EHN were introduced into the reservoir by a syringe. The weight of the liquid fuel introduced into the reservoir was determined as the difference in weight of the syringe before and after the introduction. The uncertainty in weight of liquid fuel was about 5% which resulted in an uncertainty in mole fraction of

HN within the mixtures of about 5%. Table 1 summarizes the composition of gas mixtures investigated in this study. The temperature of the reservoir was maintained at 80 °C to ensure the total vaporization of the liquid fuels. For each gas mixture, a mechanic agitation during 30 minutes was conducted to ensure the homogeneity. All gas mixtures were prepared on the day of manipulation.

**Table 1**

Composition in molar basis of gas mixtures in RCM experiments.

Mix.	Toluene (%)	n-Heptane (%)	HN (ppm)	O <sub>2</sub> (%)	N <sub>2</sub> (%)
Neat surrogate	1.54	0.61	-	20.55	77.30
HN 0.1%	1.54	0.60	21.5	20.55	77.30
HN 1%	1.53	0.60	214.9	20.55	77.30

For each IDT measurement, the pressure at the top dead center ( $P_c$ ) and the temperatures at top dead center ( $T_c$ ) were obtained by regulating the intake pressure ( $227 \text{ mbar} < P_0 < 600 \text{ mbar}$ ) and the piston initial temperature ( $55 \text{ }^\circ\text{C} < T_0 < 120 \text{ }^\circ\text{C}$ ). The maximum deviation of  $P_c$  between different measurements was 0.8 bar. The  $T_c$  are calculated thanks to the isentropic relation, where  $\gamma$  is the ratio of specific heats of gas mixture:

$$\int_{T_0}^{T_c} \frac{\gamma}{\gamma - 1} \frac{dT}{T} = \ln \left( \frac{P_c}{P_0} \right) \quad (1)$$

In this study, the main IDT is defined as the time between the end of the compression and the combustion Maximum Pressure Rise Rate (MPRR), which corresponds to the peak of the  $dP/dt$  profile. In the case of two-stage ignitions, the 1<sup>st</sup>-stage IDT is determined as the time between the end of compression and the first distinguishable peak of  $dP/dt$ . Under each condition of IDT measurement, very good repeatability of  $P_c$  is observed as presented in Figure 1. The range of measurable IDT by

this RCM is between 1 and 200 ms. The longest delay measured in this study is about 50 ms. After each experiment with doped fuels, the interior surfaces of equipment including the mixing tank, feed lines, and valves were carefully cleaned by flux of air. For each experimental condition including the doped and the undoped fuels, six tests were repeated. For example, for the neat fuel, three successive tests were performed before using the doped fuel and three after. The uncertainty in  $T_c$  is about 3 K. The uncertainty in IDT vary with the IDT. For IDT below 10 ms, the uncertainty is about 0.5 ms. In the case of higher IDT ( $> 10$  ms), the uncertainty varies from 1 to 2 ms and within this range it increases with IDT. As a good repeatability was obtained, it was confirmed that the measurements were not fouled by the adsorption of EHN on the interior surface of the equipment.

(A)

(B)

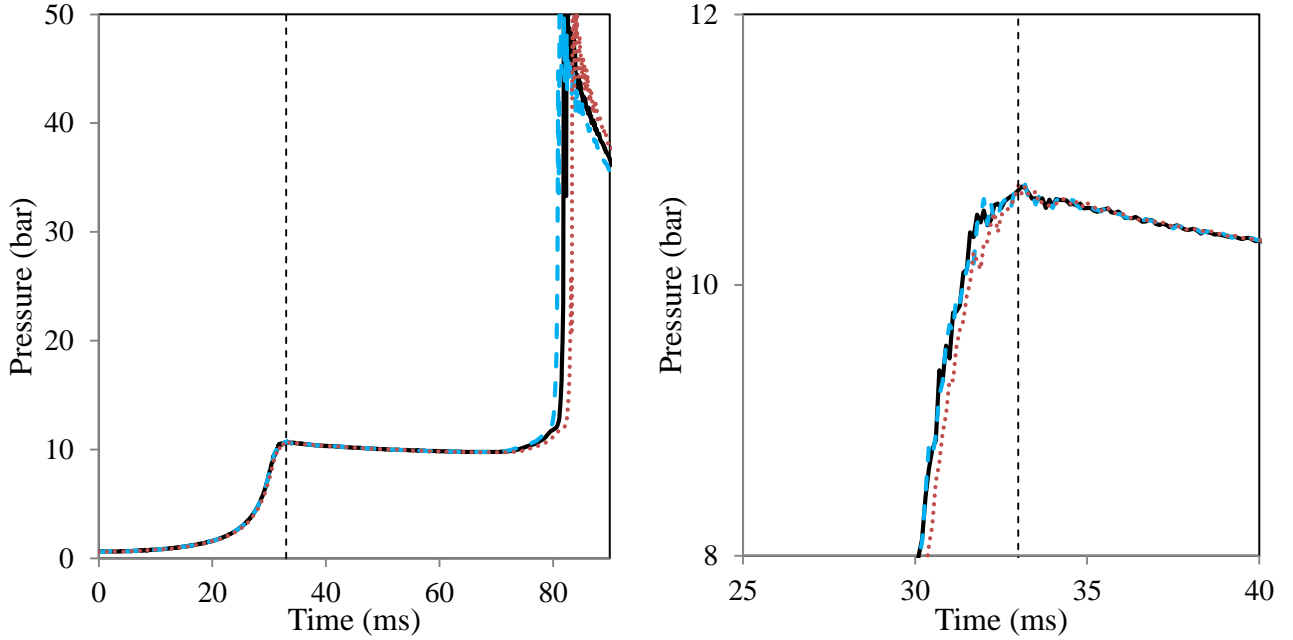


**Figure 1.** Pressure histories of three successive RCM tests (solid lines, dashed lines, and dash-dotted lines) for the neat surrogate fuel at  $P_c = 10$  bar,  $T_c = 675$  K,  $\Phi = 1$ . End of compression: vertical dashed line. (A): whole range of time. (B): zoom in the range of time near the end of compression.

### 3. Kinetic modeling

#### 3.1. Kinetic model assembling and RCM simulation methods

A detailed kinetic model was developed in this work to understand the effect of EHN on the surrogate fuel reactivity. The surrogate fuel mechanism was adopted from a previous study [19]. This mechanism was built from the kinetic model of Lawrence Livermore National Laboratory (LLNL) [26] with updating the toluene sub-mechanism from recent data in the literature [27–31]. The detail of the construction of the surrogate fuel mechanism can be found elsewhere [19].

The past studies of EHN [16,18,32] agree on the main decomposition steps of this molecule. At first,  $\text{NO}_2$  is released thanks to N-O bond scission, which is the weakest bond in EHN molecule. Together with  $\text{NO}_2$ , the 2-ethylhexyloxy (EHO) radical is formed. The detail chemistry of EHO is still unknown. A recent study of *n*-butyl nitrate (NBN) thermal decomposition was conducted by Morin et

al. [33]. NBN decomposition formed butoxy radical ( $C_4H_9O$ ) and  $NO_2$ . The most favorable channels for  $C_4H_9O\cdot$  transformation were its decomposition to propyl radical ( $C_3H_7$ ) and formaldehyde ( $CH_2O$ ) and its isomerization to hydroxybutyl radical ( $C_4H_8OH$ ). Interestingly, the dominant transformation of  $C_4H_8OH$  was its back isomerization to  $C_4H_9O$  and then decomposition to  $C_3H_7$  and  $CH_2O$ . The NBN decomposition can be described as a global reaction  $NBN \rightarrow C_3H_7 + CH_2O + NO_2$ . A similar reaction is then adopted in this study to describe the decomposition of EHN as presented in Table 2. The decomposition products of EHN are 3-heptyl radical ( $C_7H_{15}-3$ ),  $CH_2O$  and  $NO_2$ . The rate constant of this reaction is estimated according to the experimental works on EHN decay of Pritchard et al. [34] and Bornemann et al. [32].

**Table 2**

Kinetic constant of EHN decomposition reaction

Reaction	A	n	$E_a$	Ref.
$EHN \rightarrow C_7H_{15}-3 + CH_2O + NO_2$	$2.50 \times 10^{15}$	0	42000	[32,34]

Rate expression:  $k = AT^n \exp\left(\frac{-E_a}{RT}\right)$  in  $\text{cm}^3$ , mol, cal, s units.

Different studies on EHN in literature showed different explanations of EHN impact on fuel reactivity. Hartmann et al. [16] suggested that EHN effect linked to the chemical reactivity of 3-heptyl radical. Goldsborough et al. [18] indicated that together with 3-heptyl radical, a “ $NO_2$ -NO” loop involving reactions of nitrogen oxides ( $NO_x$ ) with small radicals ( $H$ ,  $HO_2$ ) could generate OH radicals contributing to the EHN effect. Recent study [19] of EHN promoting effect on aromatic fuel revealed that  $NO_2$  could react with primary radical derived from fuel to enhance the fuel reactivity. These explanations of EHN effect suggest that the detail nitrogen chemistry including interactions with heavy

hydrocarbon ( $> \text{C}_3$ ) must be considered to better simulate EHN promoting effect. Consequently, the kinetic model in this study includes a detail nitrogen chemistry mechanism developed and validated against literature data. The  $\text{NO}_x$  sub-mechanism including light hydrocarbons ( $\text{C}_1\text{-}\text{C}_2$ ) was collected from the recent review of Glarborg et al. [35] and the work of Fuller et al. [36]. The reactions of nitroethane presented in the work of Zhang et al. [37] were used. The reactivity of the two nitropropane isomers (1-nitropropane and 2-nitropropane) was built based on the reaction scheme of nitroethane. The interactions between  $\text{NO}_x$  and heavy hydrocarbons ( $\text{C}_4\text{-}\text{C}_7$ ) were adopted from the study of Anderlorh et al. [38]. The sensitizing effect of  $\text{NO}_x$  on hydrocarbon oxidation has been investigated in the literature [39–43]. These studies highlighted the importance of reactions  $\text{R} + \text{NO}_2 = \text{RO} + \text{NO}$  and  $\text{RO}_2 + \text{NO} = \text{RO} + \text{NO}_2$  on the sensitizing effect of  $\text{NO}_x$ . The most important reactions of  $\text{NO}_x$  impacting the oxidation of *n*-heptane and toluene are presented in Table 3. The rate constant of reaction R2 between  $\text{HO}_2$  and NO was first experimentally measured over a wide range of temperature 232 – 1271 K in a flow tube reactor by Howard et al. [44]. The rate constant reported by these authors was  $k = 2.11 \times 10^{12} \times \exp(477/RT)$  (units: cal, mol, s, K). This result was supported by the more recent experimental study of Bardwell et al. [45] and the theoretical study of Chen et al. [46]. Bardwell et al. [45] conducted experiments in a turbulent flow tube at low temperatures 183–300 K in a pressure range of 75 to 220 Torr. The rate constant of R2 was found pressure independent and agreed well with the rate reported by Howard et al. [44]. Chen et al. [46] determined the reaction pathway of R2 at 300 K thanks to quasi-classical trajectory calculations. HOONO was found to be the principal intermediate

which further decayed into NO<sub>2</sub> and OH. The calculated rate constant of R2 at 300 K was in good agreement with the measurement reported by Howard et al. [44]. In our model, the rate constant of R2 reported in the review of Glarborg et al. [35] is adopted. This value is included in the uncertainty range of the rate constant reported in [44]. The rate constant of reaction R3 between CH<sub>3</sub>O<sub>2</sub> and NO was both experimentally and theoretically investigated in the literature. Bacak et al. [47] measured the global rate constant of the reaction CH<sub>3</sub>O<sub>2</sub> + NO<sub>2</sub> → *Products* in a turbulent flow tube reactor from 193 to 300 K in a pressure range of 100 to 200 Torr. These authors reported a rate constant  $k = 1.05 \times 10^{12} \times \exp(864/RT)$  (units: cal, mol, s, K). The branching ratio of the formation of CH<sub>3</sub> and NO<sub>2</sub> was found to be  $100 \pm 10\%$ . This result was supported by the study of Butkovskaya et al. [48]. These authors tried to experimentally determine the branching ratio of methyl nitrate formation in the CH<sub>3</sub>O<sub>2</sub> + NO reaction. The experiments were conducted in turbulent flow reactor over the pressure and temperature ranges 50 – 500 Torr and 223 – 300 K, respectively. The branching ratio of methyl nitrate formation was determined as a value of 1 % in the considered conditions. Also, the theoretical study of Lesar et al. [49] confirmed the most dominant products of CH<sub>3</sub>O<sub>2</sub> + NO reaction were CH<sub>3</sub>O and NO. In our model, the rate constant of R3 reported in the review of Glarborg et al. [35] is adopted. This value is similar to the global rate constant reported by Bacak et al. [47]. The rate constant of reaction R4 between C<sub>2</sub>H<sub>5</sub>O<sub>2</sub> and NO was experimentally measured by Maricq et al. [50] over the temperature range 220 – 335 K. These authors reported a A-factor and an activation energy (E<sub>a</sub>) of  $1.87 \times 10^{12} \pm 9 \times 10^{11}$  and  $-656 \pm 217$  respectively (units: cal, mol, s, K). This result was supported by

the experimental work of Ranschaert et al. [51]. These authors determined also the minor formation of ethylnitrate whose branching varied from 0.006 to 0.02. In our model, the rate constant of R4 proposed in the model of Rasmussen et al. [42] is adopted. This value is included in the uncertainty range of the rate constant reported in [50]. To our knowledge, the rate constant of reaction R5 between C<sub>7</sub>H<sub>15</sub>O<sub>2</sub> and NO was not directly examined in the literature. In our model, the rate constant of R5 is adopted from the model of Anderlohr et al. [38]. These authors estimated this rate constant by multiplying the rate constant rate of reaction CH<sub>3</sub>O<sub>2</sub> and NO reported in [52] by a factor of 1.8. Also, no data in the literature are found for the reaction R1 between C<sub>6</sub>H<sub>5</sub>CH<sub>2</sub> and NO<sub>2</sub>. The rate constant of this reaction is based on the rate constant of the reaction of alkyl radicals (R) with NO<sub>2</sub>: R + NO<sub>2</sub> = RO + NO proposed by Anderlohr et al. [38].

**Table 3**

Rate coefficients of reactions of NO<sub>x</sub>

Reaction	A	n	E <sub>a</sub>	A-factor	Ref.
----------	---	---	----------------	----------	------

						modification
Reactions of R/RO <sub>2</sub> + NO <sub>x</sub>						
<b>R1</b>	C <sub>6</sub> H <sub>5</sub> CH <sub>2</sub> + NO <sub>2</sub> = C <sub>6</sub> H <sub>5</sub> CH <sub>2</sub> O + NO	4.00 x 10 <sup>13</sup>	0.00	0		This work
<b>R2</b>	HO <sub>2</sub> + NO = OH + NO <sub>2</sub>	2.05 x 10 <sup>12</sup>	0.00	-497		[35]
<b>R3</b>	CH <sub>3</sub> O <sub>2</sub> + NO = CH <sub>3</sub> O + NO <sub>2</sub>	1.40 x 10 <sup>12</sup>	0.00	-715		[35]
<b>R4</b>	C <sub>2</sub> H <sub>5</sub> O <sub>2</sub> + NO = C <sub>2</sub> H <sub>5</sub> O + NO <sub>2</sub>	1.60 x 10 <sup>12</sup>	0.00	-755		[42]
<b>R5</b>	C <sub>7</sub> H <sub>15</sub> O <sub>2</sub> + NO = C <sub>7</sub> H <sub>15</sub> O + NO <sub>2</sub>	4.70 x 10 <sup>12</sup>	0.00	-358		[38]
<b>R6</b>	NO <sub>2</sub> + HO <sub>2</sub> = O <sub>2</sub> + HONO	3.65 x 10 <sup>13</sup>	0.00	8000		[46]
<b>R7</b>	NO <sub>2</sub> + CH <sub>2</sub> CHO = CH <sub>2</sub> CO + HONO	2.00 x 10 <sup>15</sup>	-0.68	1430		[35]
<b>R8</b>	C <sub>2</sub> H <sub>5</sub> NO <sub>2</sub> = C <sub>2</sub> H <sub>5</sub> + NO <sub>2</sub>	8.61 x 10 <sup>63</sup>	-14.48	77543		[37]
Reactions of RCHO + NO <sub>2</sub>						
<b>R9</b>	CH <sub>3</sub> CHO + NO <sub>2</sub> → CH <sub>3</sub> + CO + HONO	4.20 × 10 <sup>-10</sup>	6.68	8300	× 5	[38]
<b>R10</b>	C <sub>2</sub> H <sub>5</sub> CHO + NO <sub>2</sub> → C <sub>2</sub> H <sub>5</sub> + CO + HONO	4.20 × 10 <sup>-10</sup>	6.68	8300	× 5	[38]
<b>R11</b>	n-C <sub>3</sub> H <sub>7</sub> CHO + NO <sub>2</sub> → n-C <sub>3</sub> H <sub>7</sub> + CO + HONO	4.20 × 10 <sup>-10</sup>	6.68	8300	× 5	[38]
<b>R12</b>	n-C <sub>4</sub> H <sub>9</sub> CHO + NO <sub>2</sub> → n-C <sub>4</sub> H <sub>9</sub> + CO + HONO	4.20 × 10 <sup>-10</sup>	6.68	8300	× 5	[38]
<b>R13</b>	n-C <sub>5</sub> H <sub>11</sub> CHO + NO <sub>2</sub> → n-C <sub>5</sub> H <sub>11</sub> + CO + HONO	4.20 × 10 <sup>-10</sup>	6.68	8300	× 5	[38]

Rate expression:  $k = AT^n \exp\left(\frac{-E_a}{RT}\right)$  in cm<sup>3</sup>, mol, cal, s units.

In simulations, it was also found that the reactions of aldehydes with NO<sub>2</sub> (R9 – R13) were sensible to predict the effect of NO on *n*-heptane oxidation. The kinetic of this type of reactions were estimated by Anderlorh et al. thanks to the reaction of CH<sub>2</sub>O and NO<sub>2</sub> calculated by Xu et al. [53]. The A-factor of the reactions of aldehydes with NO<sub>2</sub> proposed by Anderlohr et al. were multiplied by 5 in order to better simulate the impact of NO on *n*-heptane oxidation presented in the study of Moréac et al. [54]. The modified reactions are presented in Table 3. The resulting model includes 1686 species and 7817 reactions. This model is provided in Supplementary Data.

A recent review of RCM studies by Goldsborough et al. [7] indicates that IDT measured in a RCM can be simulated by using a homogenous reactor model with two common approaches. The first method named “frozen chemistry” assumes no reactions occur during the compression process of

RCM tests. The thermodynamic inputs of this simulation method are conditions ( $P_c$ ,  $T_c$ ) at the top dead center. The second method entitled “all-simu” considers the chemical reactivity of gas mixture during the piston movement. The intake pressure ( $P_0$ ) and the piston initial temperature ( $T_0$ ) are used as the initial thermodynamic conditions for modeling. The heat loss during a RCM test is taken into account by using an “effective volume” for both two simulation methods. This corresponds to a volume profile obtained by conducting non-reactive experiments where  $O_2$  is replaced by  $N_2$ . This implies that the initial conditions ( $P_0$ ,  $T_0$ ) are similar to those of reactive experiments. The non-reactive pressure trace is then used in a calculation of the adiabatic core hypothesis to deduce the volume profile as described by Tanaka et al. [55]. In this work, the “all-simu” method was adopted to better capture the EHN promoting effect and to discuss the EHN action during compression process. The simulation results obtained thanks to the 0-D closed homogenous reactor model in CHEMKIN-PRO [56] are discussed further in this paper.

### *3.2. Kinetic model validation*

The developed kinetic model was validated using a large set of experimental data. This includes ignition data in shock tube (ST) as well as species profiles measured in plug flow reactor (PFR) and perfectly stirred reactor (PSR). The comparison was performed to validate different sub-mechanisms: the toluene/ *n*-heptane mixtures reactivity [25,57], the nitrogen chemistry [37,42,43,54,58–62] and the effect of EHN [16]. The used experimental data are presented in Table 4.

**Table 4**

Summary of experimental studies used for the validation of the kinetic mechanism

Reactor	Fuel	Equivalence ratio	Temperature (K)	Pressure (atm)	Ref.
<b>PFR<sup>a</sup></b>					
	Methane/ NO/ NO <sub>2</sub>	1.20	600-900	50	[42]
	Methane/ NO <sub>2</sub>	4.00	870-1225	2	[58]
	Nitroethane	pyrolysis	680-1425	$7 \times 10^{-3}$	[37]
<b>PSR<sup>b</sup></b>					
	Ethane/ NO	1.00	825-1100	1	[43]
	<i>n</i> -Heptane/ NO	1.00	550-1000	10	[54]
	Toluene/NO	1.00	640-1100	10	[54]
	Toluene/ <i>n</i> -heptane/NO/NO <sub>2</sub>	0.2	550-950	10	[59]
<b>ST<sup>c</sup></b>					
	Nitromethane	pyrolysis	1180	6	[60]
	Nitromethane	1.00-2.00	875-1110	9-14	[61]
	2-Nitropropane	pyrolysis	975-1100	5	[62]
	Toluene/ <i>n</i> -heptane	0.30-1.00	840-1200	10-50	[25]
	Toluene/ <i>n</i> -heptane	1.00	710-1200	40	[57]
	<i>n</i> -heptane/ EHN	1.00	700-1200	40	[16]

<sup>a</sup> Plug flow reactor. <sup>b</sup> Perfectly stirred reactor. <sup>c</sup> Shock tube.

The validation step confirms a good performance of the kinetic model to reproduce the reactivity of toluene and *n*-heptane mixtures as presented in a previous study [19]. The model reliably predicts the NO<sub>x</sub> effect on fuel reactivity. Moréac et al. [54] studied the impact of NO on the oxidation of *n*-heptane and toluene by conducting experiments at 10 atm from 550 to 1090 K in a PSR. Figure 2 presents the modeling results for this data set.

(A)

(B)

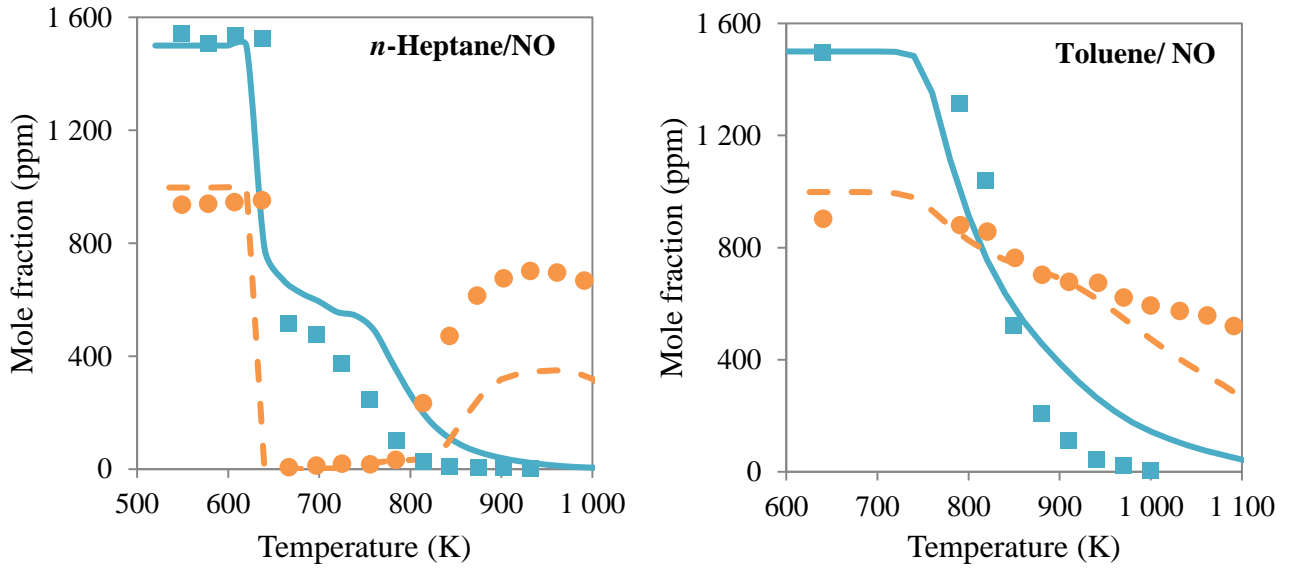


**Figure 2.** Species profiles of fuel (solid lines and square symbols) and NO  $\times$  2 (dashed lines and circle symbols) at 10 atm from 500 to 1100 K. Symbols: experimental results. Lines: simulations results. (A): initial fuel mixture: *n*-heptane/ 500 ppm NO. (B) initial fuel mixture: toluene/ 500 ppm NO. Experiments conducted by Moréac et al.[54].

Figure 3 illustrates the modeling of the ignition delays for *n*-heptane doped with 1% mass. EHN at 40 bar and  $\Phi = 1$ . While the mechanism accurately captures the change in ignition delays upon doping EHN, the predicted the ignition delays of the doped and undoped mixtures at lower temperatures ( $T < 1000$  K) were found to show some differences with the simulated IDTs being larger than experimental measurements by about 50%.

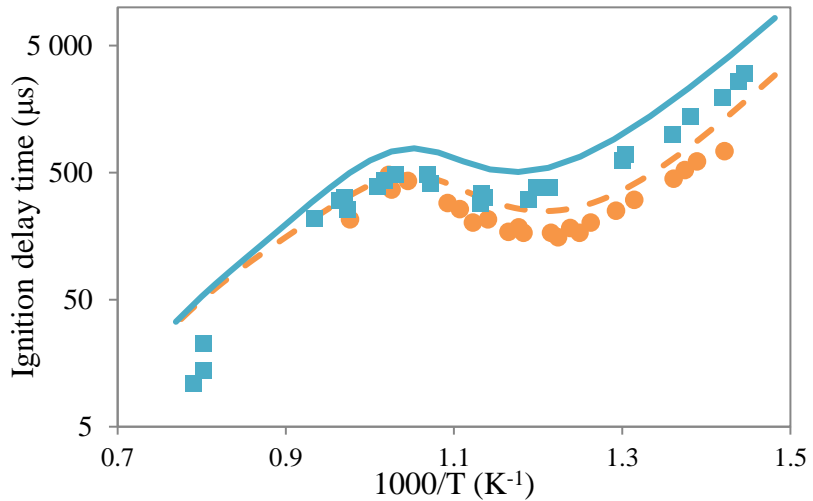


**Figure 3.** Measured (symbols) and simulated IDT (lines) of the neat *n*-heptane (solid line and square symbols) and doped *n*-heptane with 1% mass EHN (dashed line and circle symbols) at  $P = 40$  bar,  $\Phi = 1$ . Experiments conducted by Hartmann et al.[57].

The modeling of other experimental data listed in Table 4 are presented in Supplementary Data.

The validation step demonstrates a satisfactory agreement regarding the entire data set employed.

#### 4. Results and Discussions

The experimental and modeling results are presented in this section. First, the measured and simulated IDT of the neat surrogate fuel are displayed. Then the EHN promoting effect on the surrogate fuel reactivity is shown. Thanks to the validated model, the EHN decomposition during the compression process of RCM tests and the EHN promoting effect as a function of the equivalence ratio are discussed. Eventually, the chemical reactions involved in the EHN effect are analyzed numerically.

##### 4.1 IDT of the surrogate fuel

RCM experiments were performed at 10 bar from 675 to 960 K for stoichiometric mixtures in air.

The ignition delays of the surrogate fuel without additive are presented in Figure 4. NTC is observed

from 790 K to nearly 885 K while two-stage ignitions occur in the lowest temperature range ( $T_c < 790$  K). *n*-Heptane oxidation enables this feature as described by Battin-Leclerc et al. [63]. The simulation reasonably reproduces the RCM experimental results including two-stage ignitions and NTC phenomenon. The 1<sup>st</sup>-stage IDT are underestimated by a factor of two (a factor of five at the lowest  $T_c = 675$  K). The main IDT at the lowest temperatures ( $T_c < 790$  K) are underestimated by 20 % while the main IDT in the upper temperature range ( $T_c > 790$  K) is correctly simulated. Globally, the surrogate fuel reactivity is well captured by the proposed kinetic model.

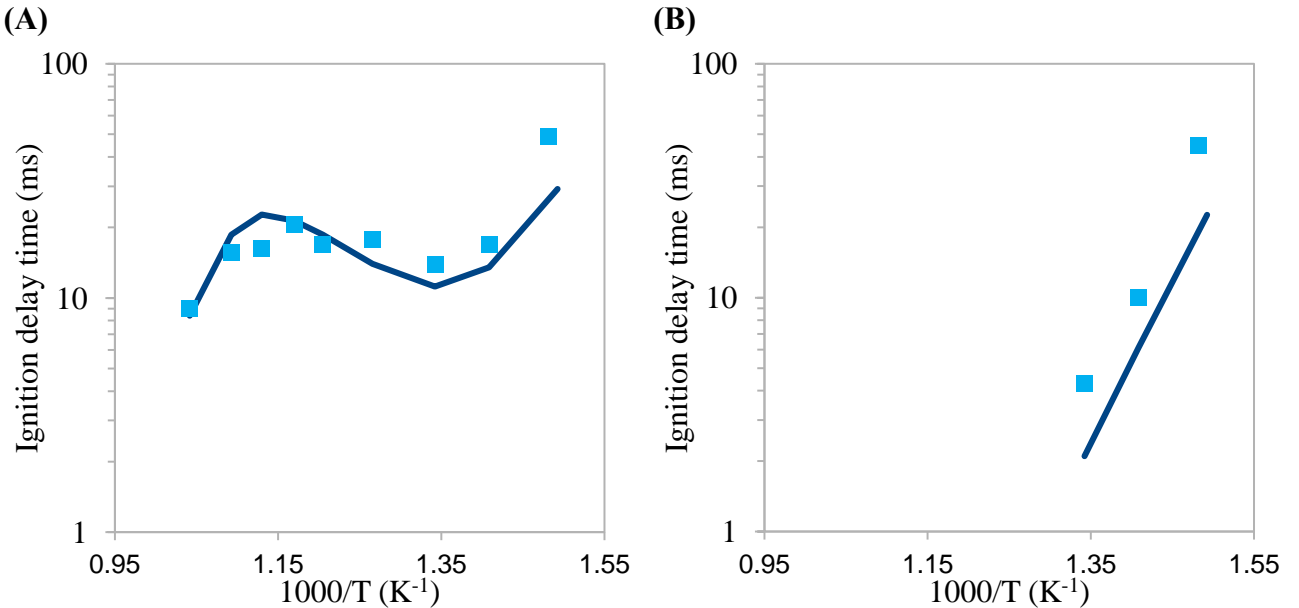


**Figure 4.** Measured ignition delay times of the surrogate fuel at 10 bar and  $\Phi = 1$ . Experiments: square symbols. Simulation: solid lines. (A) Main IDT , (B) 1<sup>st</sup>-stage IDT.

#### 4.2 IDT of the fuel doped with EHN

Goldsborough et al. [18] demonstrated that under some conditions, the gas mixtures doped with EHN released a remarkable heat during the compression process. A similar trend appears in this study. Under similar experimental conditions for the surrogate fuel and with 0.1 % mol. of EHN, a heat

release before then end of the compression is recorded when the additive is used. This is characterized by a significant pressure increase compared to the measurement with the neat surrogate fuel. An evaluation of  $T_c$  by the adiabatic calculation for these experiments may lead to an important bias. In order to be consistent,  $T_c$  shall only correspond to the experiments with the undoped fuel mixtures. Figure 5 illustrated the EHN effect on the fuel surrogate IDT. Nevertheless, attention must be paid to understanding Figure 5. For example, the experimental  $T_c$  reached by the compression of the surrogate fuel doped with 1% EHN at nominal conditions ( $T_c = 960$  K,  $P_c = 10$  bar) is higher than 960 K due to the exothermic reaction, but cannot be determined without numerical simulation by the adiabatic unreactive compression calculation.

(A)

(B)

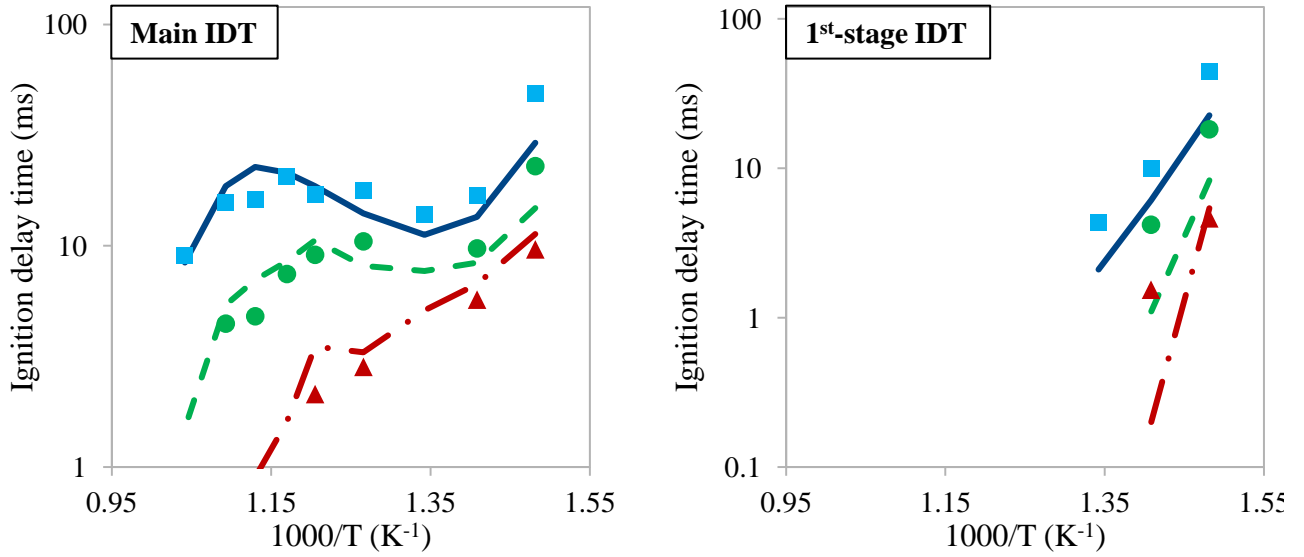


**Figure 5.** Measured and simulated 1<sup>st</sup>-stage and main IDT of the neat and doped fuels. Symbols refer to experimental data and lines are used to illustrate modeling work. The neat surrogate fuel results are illustrated with solid lines and square symbols. Doped fuels with 0.1% EHN is presented with dashed lines and circle symbols and 1% EHN with dash-dotted lines and triangle symbols. (A) Main IDT , (B) 1<sup>st</sup>-stage IDT.

At the investigated experimental conditions (10 bar,  $\Phi = 1$ ), EHN promotes the reactivity of the fuel at all examined  $T_c$  (675 – 960 K). A significant reduction of both 1<sup>st</sup>-stage IDT and main IDT of the surrogate fuel is observed in presence of EHN. This effect increases with EHN doping levels. The NTC behavior of the surrogate fuel is mitigated by the addition of EHN. At doping level of 1% mol., EHN suppresses totally the NTC behavior. The EHN promoting effect is least significant at temperatures 710 - 745 K and then increases with  $T_c$ . This feature is similar to the observation of Goldsborough et al. [18], which indicated that EHN had the weakest influence on the reactivity of the primary reference fuel (blend of *n*-heptane and iso-octane) of RON 91 and toluene reference fuel (blend of *n*-heptane, iso-octane and toluene) of RON 91 near 740 K.

The promoting effect of EHN according to compression temperatures and doping levels is well

predicted by the kinetic model. The 1<sup>st</sup>-stage IDT of the doped fuels is slightly underestimated in simulations which is also observed for the neat fuel. The main IDT modelling of the doped fuels are in good agreement with the experimental ones. Figure S11 in Supplementary Data presents the simulated IDT of the neat and doped surrogate fuel by adopting the “frozen chemistry” method. It was observed that the “frozen chemistry” method underestimated largely the EHN promoting effect in the considered conditions of this study. This confirms that the “all-simu” method is appropriate to simulate IDT of high reactivity fuels measured in RCM as suggested in the litterature [9].

In order to capture the early heat release due to EHN addition, the simulations were further analyzed. Figure 6 presents the simulated species profiles and the simulated pressure history during RCM tests at  $T_c = 675$  K (A) and  $T_c = 915$  K (B). At low  $T_c$  (675K), EHN decomposes slightly before the end of compression. The decomposition of EHN progresses gradually until the 1<sup>st</sup>-stage ignition time where EHN is rapidly consumed. At high  $T_c$  (915 K), EHN decomposes totally before the end of piston movement. At  $T_c = 675$  K, the gas mixture temperature increases gradually thanks to the heat release from the surrogate fuel oxidation after the end of the compression. However, for the condition  $T_c = 915$  K, the compression increases the gas temperature leading to the full decay of EHN when the temperature reaches 830 K, before the piston stops. The reaction of the surrogate fuel, i.e. the toluene / *n*-heptane blend, is then initiated, which results in an increase of  $P_c$ . This is validated thanks to the simulation of pressure histories near the end of the compression of RCM experiments (see Figure 7). It was experimentally found that at  $T_c = 675$  K, there is no  $P_c$  change in both the undoped and doped

fuel tests. However, at  $T_c = 915$  K, the  $P_c$  increases remarkably in the presence of EHN 0.1% mol.

These features are well captured by the developed kinetic model.

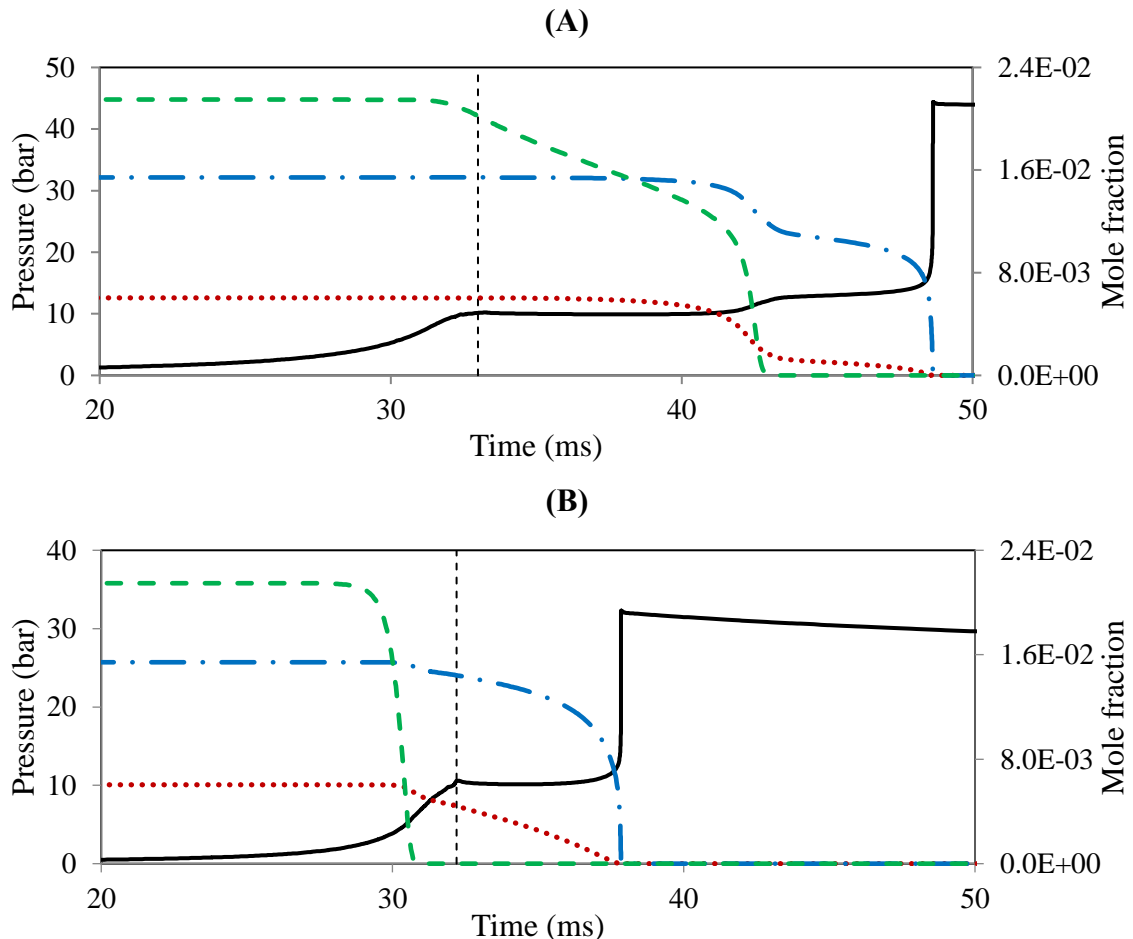


**Figure 6.** Simulated species profiles of toluene (dash-dotted lines), *n*-heptane (dotted lines), EHN  $\times$  1000 (dashed lines) and simulated pressure histories (solid lines) of RCM experiments at  $P_c \approx 10$  bar,  $\Phi = 1$  and 0.1% mol. EHN. (A):  $T_c = 675$  K and (B):  $T_c = 915$  K. End of compression: vertical dashed lines.

(A)

(B)

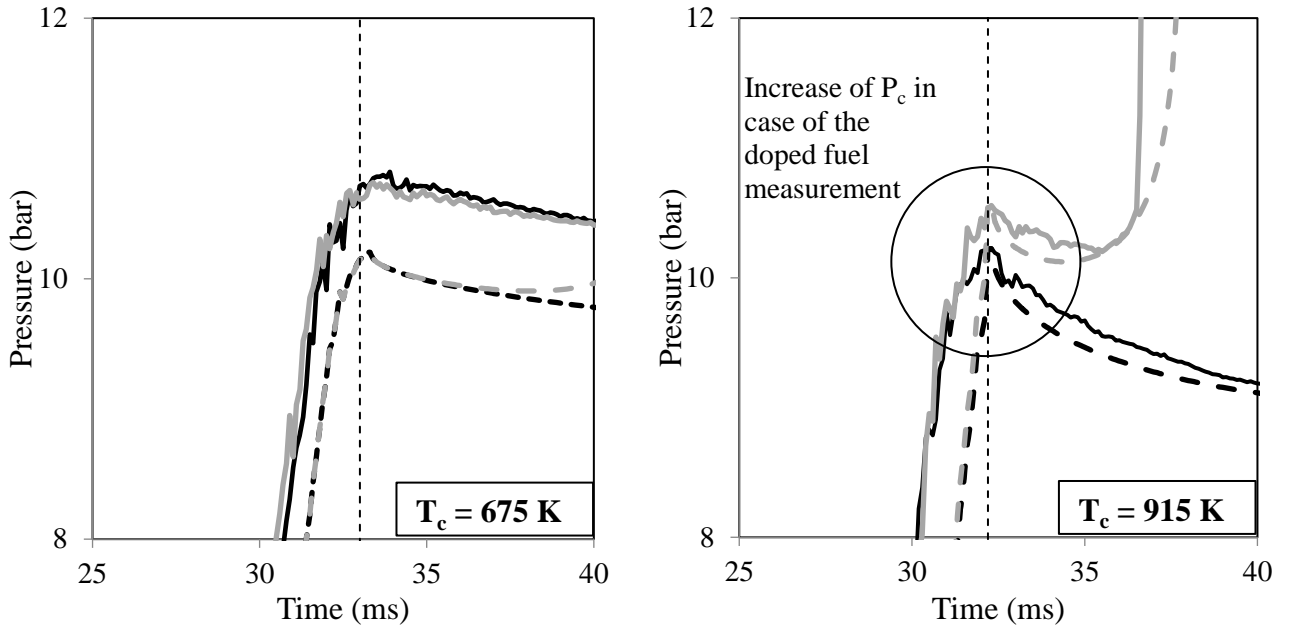


**Figure 7.** Measured (solid line) and simulated (dashed line) of pressure histories near the top dead center during RCM experiments at  $P_c \approx 10$  bar,  $\Phi = 1$  of the neat surrogate fuel (black) and the surrogate fuel doped with EHN 0.1% mol (grey). (A):  $T_c = 675$  K and (B):  $T_c = 915$  K. End of compression: dashed black line.

As observed in Figure 5, the promoting effect of EHN evaluated in RCM tests rises with  $T_c$ . As  $T_c$  increases, EHN decomposes earlier during the compression process. The chemical reactivity of gas mixture during the compression process is higher, which results in a shorter IDT. As a consequence, the EHN promoting effect is partly linked to the compression time. Consequently, a different RCM with another compression time would produce a different EHN effect on the surrogate fuel IDT.

#### 4.3. EHN effect with various equivalence ratios

Figure 8 presents the simulations of EHN promoting effect on toluene/*n*-heptane mixture [19], which is identical to the surrogate fuel used in this study, at  $P_c = 10$  bar and  $\Phi = 0.5$ . The “all-simu” method was used to simulate RCM experiments and  $T_c$  in Figure 8 corresponding to the neat surrogate test. The kinetic mechanism simulates reasonably well the EHN promoting effect on main ignition.

The model however overestimates the EHN promoting effect on the 1<sup>st</sup>-stage ignition. By experiments, the 1<sup>st</sup>-stage ignitions were observed in the case of the fuel doped with EHN 1% at two  $T_c$ : 675 K and 705 K. The measured 1<sup>st</sup>-stage IDT at these  $T_c$  are 15.8 and 3.1 ms respectively. Meanwhile, only 1<sup>st</sup>-stage ignition at  $T_c = 675$  K was simulated (4.5 ms) by the kinetic model of this study. This may be related to the underestimation of the IDT regarding the neat surrogate under these conditions.

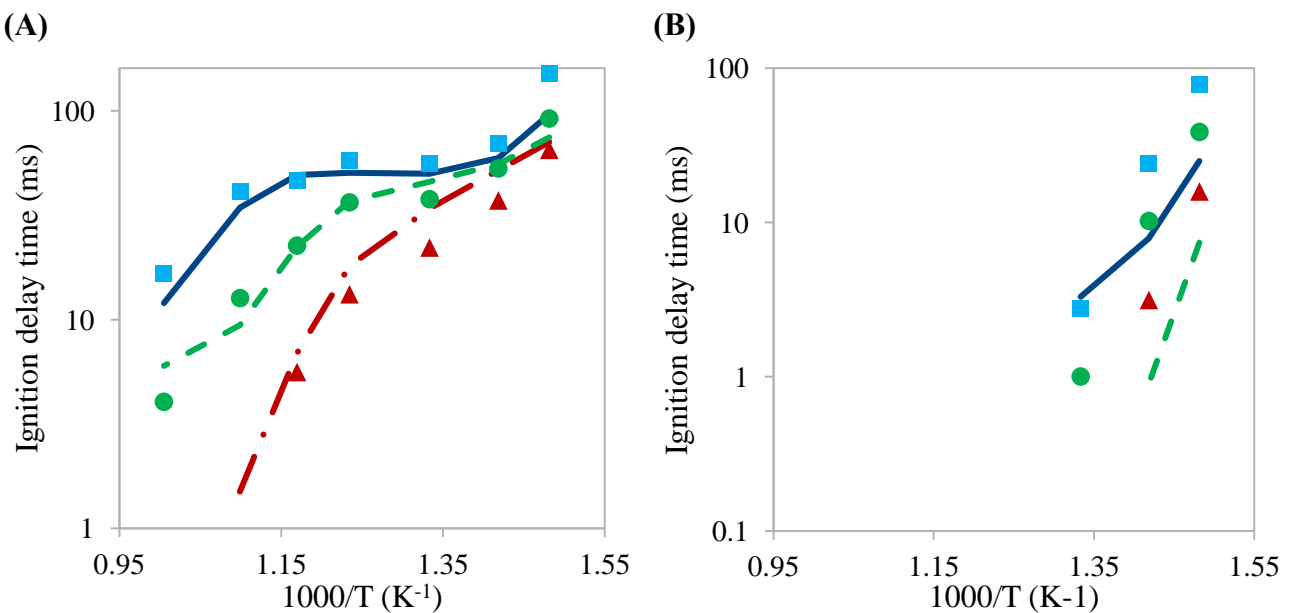


**Figure 8.** Measured (symbols) and simulated (lines) IDT of the neat surrogate fuel (solid lines and square symbols) and doped fuels with 0.1% EHN (dashed lines and circle symbols) and 1% EHN (dash-dotted lines and triangle symbols) at  $P_c = 10$  bar,  $\Phi = 0.5$ . (A) main IDT. (B) 1<sup>st</sup>-stage IDT. Experimental data collected from [19].

Figure 9 shows the simulated relative effect ( $R_{eff}$ ) of EHN (0.1% mol.) on the main ignition of the fuel surrogate at  $P_c = 10$  bar,  $T_c = 675 - 915$  K and two equivalence ratios: 0.5 and 1.  $R_{eff}$  for EHN is defined in equation (2). Higher  $R_{eff}$ , stronger is the EHN promoting effect. It is found that at two different equivalence ratios, the influence of EHN on fuel reactivity follows the same trend while  $T_c$  varies. The impact of EHN is lowest at  $T_c$  near 740 K then increases with  $T_c$ . In the upper  $T_c$  range ( $>$

850 K), EHN shows the same qualitative effect for the two equivalence ratios. However, the EHN promoting effect is significantly stronger (up to 5 times) at the lower range of  $T_c$  ( $< 800$  K) for the stoichiometric mixtures. As discussed in the section 4.2, EHN activity depends on its decomposition. At low  $T_c$ , EHN decomposes partly thanks to the heat release from the fuel oxidation. Under lean condition ( $\Phi = 0.5$ ), the surrogate fuel is less reactive than at stoichiometric condition ( $\Phi = 1$ ). Consequently, the EHN decomposition is slower under lean condition implying a less pronounced additive effect.

$$R_{eff} = \frac{IDT_{undoped\ fuel} - IDT_{doped\ fuel}}{IDT_{undoped\ fuel}} \times 100\% \quad (2)$$

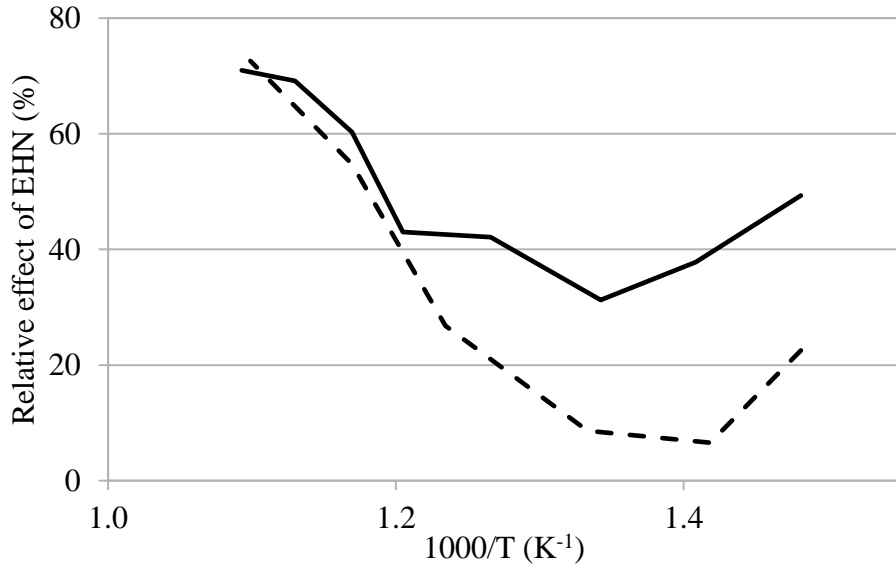


**Figure 9.** The simulated relative effect of EHN 0.1% mol. on the main IDT of the surrogate fuel) at  $P_c = 10$  bar and two equivalence ratios:  $\Phi = 0.5$  (dashed lines) and  $\Phi = 1$  (solid lines).

#### 4.4. EHN chemical effect

To understand the EHN chemical effect on the surrogate fuel, rate of production (ROP) analyses were carried out at three different  $T_c$ : 675 K, 745 K, and 915 K for EHN doping level of 0.1% mol. at

$P_c = 10$  bar and  $\Phi = 1$  during the period of EHN decomposition. As EHN decomposes quickly, the additive affects the fuel decomposition through the initiation and propagation steps. Figure 10 represents the main reaction pathways of the fuel surrogate decomposition and analyses the chemical effect of EHN. In the examined conditions, *n*-heptane reactivity follows mainly the low temperature oxidation scheme. Only at the highest  $T_c$  (915K), *n*-heptane can partly form *n*-propyl/ *n*-butyl radicals and *n*-pentyl/ ethyl radicals by unimolecular decompositions. Under this condition, heptyl radicals can undergo  $\beta$ -scission to mainly form *n*-propyl radical and *n*-butene. At the intermediate temperature ( $T_c = 745$  K), the isomers of heptyl peroxy radicals ( $C_7H_{15}OO$ ) can release  $HO_2$  radicals to form heptene. This type of reaction is one of the main reasons of NTC behavior [63]. On the other hand, toluene reactions are quite similar at all considered  $T_c$ . Toluene forms primarily benzyl radical ( $C_6H_5CH_2$ ) by H-atom abstractions. This radical can then add to  $O_2$  to form benzyl peroxy radical ( $C_6H_5CH_2OO$ ). The flux of this reaction channel was about 70% of the consumption of benzyl radicals at  $T_c = 675$  K and about 5% at  $T_c = 915$  K. Benzyl peroxy radical is not much reactive compared with isomers of heptyl peroxy radicals because of the lack of an easy intramolecular isomerization. Once formed,  $C_6H_5CH_2OO$  dominantly yields back  $C_6H_5CH_2$  by releasing  $O_2$  when temperature increases before the auto-ignition. Besides the reaction  $C_6H_5CH_2 + O_2 = C_6H_5CH_2OO$ , another important channel of  $C_6H_5CH_2$  consumption was the combination with  $HO_2$  to produce benzoxy radical ( $C_6H_5CH_2O$ ):  $C_6H_5CH_2 + HO_2 = OH + C_6H_5CH_2O$ . This radical is more reactive than the benzyl peroxy radical since it can form phenyl radical ( $C_6H_5$ ) and carbon monoxide (CO) by several H atom release steps modeled

as reactions presented in Table 5. These reactions were adopted from the recent validated toluene model of Yuan et al. [64].

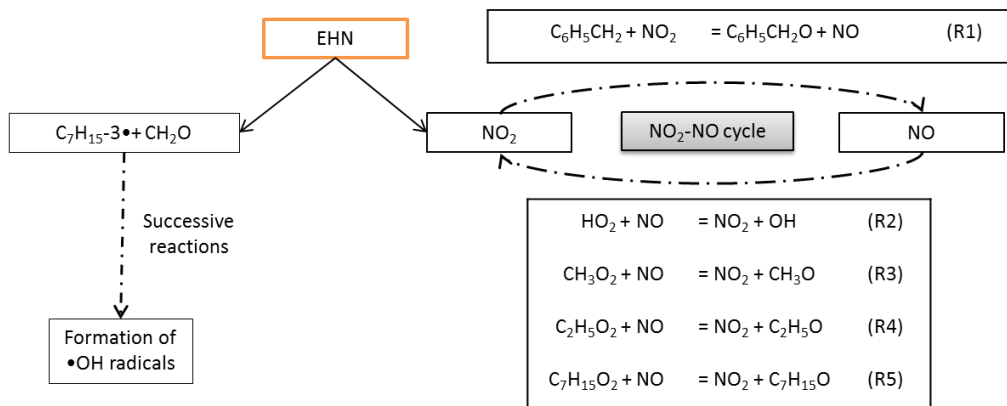
**Table 5**

Rate constants of reactions of benzoyl radical

Reaction		A	n	E <sub>a</sub>	Ref.
R <sub>I</sub>	C <sub>6</sub> H <sub>5</sub> CH <sub>2</sub> O = C <sub>6</sub> H <sub>5</sub> CHO + H	1.68 x 10 <sup>22</sup>	-2.90	20760	[65]
R <sub>II</sub>	C <sub>6</sub> H <sub>5</sub> CHO = C <sub>6</sub> H <sub>5</sub> CO + H	4.00 x 10 <sup>15</sup>	0.00	83700	[66]
R <sub>III</sub>	C <sub>6</sub> H <sub>5</sub> CO = C <sub>6</sub> H <sub>5</sub> + CO	3.98 x 10 <sup>14</sup>	0.00	29400	[66]

Rate expression:  $k = AT^n \exp\left(\frac{-E_a}{RT}\right)$  in cm<sup>3</sup>, mol, cal, s units.

### The reaction pathway of EHN



### The reaction pathway of the surrogate fuel

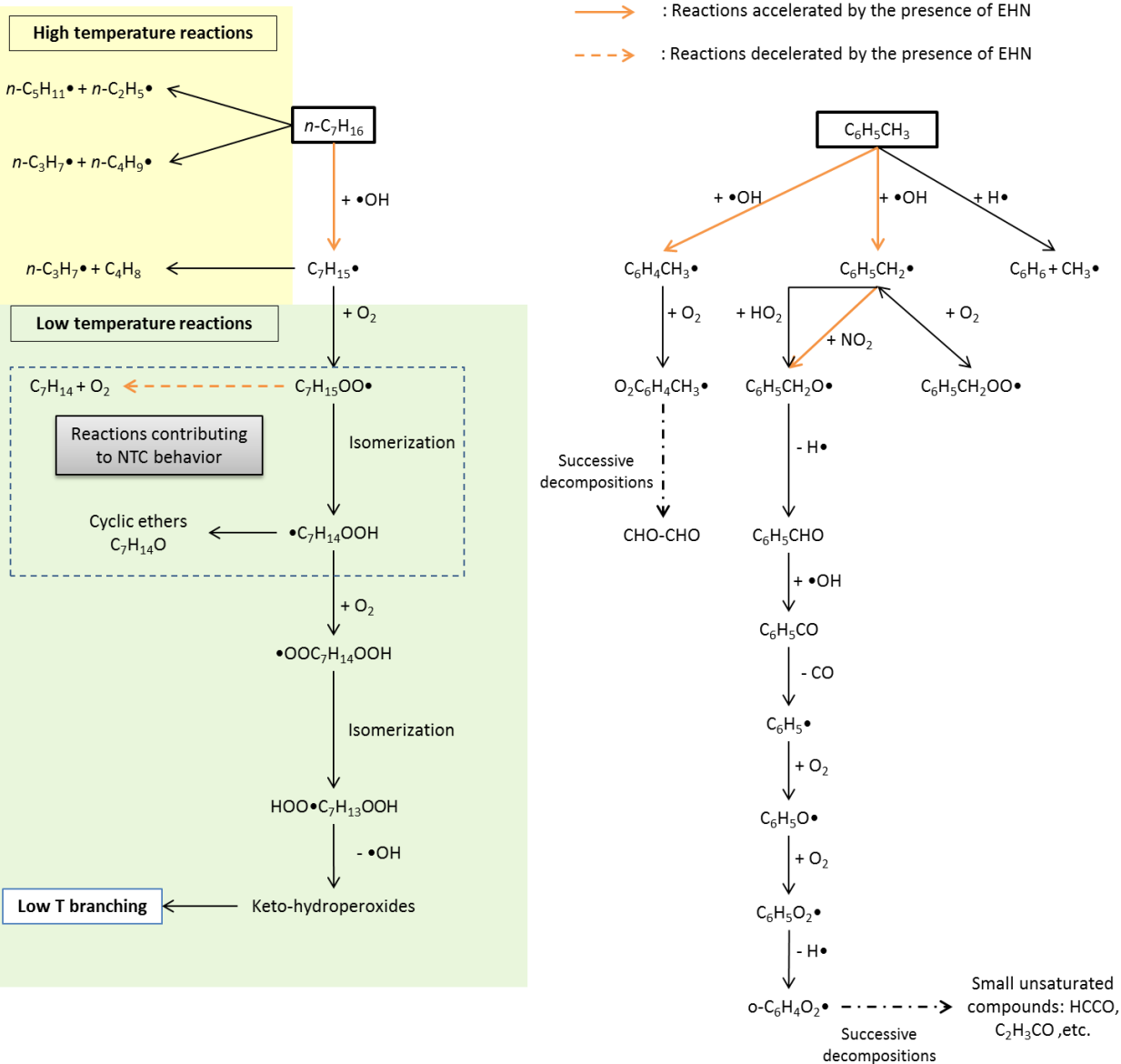


**Figure 10.** Reactions pathway of EHN and the surrogate fuel at 10 bar,  $\Phi = 1$  from 675 to 915 K

The effect of EHN lies in the chemical activity of its decomposition products C<sub>7</sub>H<sub>15</sub>-3• radical and NO<sub>2</sub>. C<sub>7</sub>H<sub>15</sub>-3• radical follows the chemical scheme presented in Figure 10 to form OH radicals, which enhances the H-atom abstractions from fuel. NO<sub>2</sub> is able to enhance toluene reactivity. NO<sub>2</sub> reacts with benzyl radical to form benzoxy radical (reaction R1). As discussed above, the last radical is more reactive than the benzyl peroxy radical thanks to its facilitated decomposition. In addition to reaction R1, NO<sub>2</sub> can follow several H-abstraction reactions with small species such as HO<sub>2</sub> and CH<sub>2</sub>CHO to form HONO (reaction R6, R7 respectively) at low T<sub>c</sub> (675 K, 745 K). Especially, at T<sub>c</sub> = 745 K, NO<sub>2</sub> is slightly stored in nitroethane (C<sub>2</sub>H<sub>5</sub>NO<sub>2</sub>) as presented in reaction R8. This is the reason why the EHN promoting effect is lowest at T<sub>c</sub> around 745 K.



The nitric oxide (NO) formed by reaction R1 can react with peroxy radicals (reactions R2 – R5) to produce NO<sub>2</sub> and the corresponding alkoxy radicals. A cycle NO<sub>2</sub> – NO is then established. At intermediate temperature (T<sub>c</sub> = 745 K), the reaction R5 competes with the HO<sub>2</sub> release reaction of the heptyl peroxy isomer radicals. Consequently, the NTC behavior is mitigated.

HN effect lies on interactions of NO<sub>x</sub> with primary radicals derived from toluene and *n*-heptane. Consequently, it is suggested that the interaction between NO<sub>x</sub> and a fuel should be carefully considered to predict the EHN promoting effect on this fuel oxidation.

In addition to ROP, sensitivity analyses on the formation of OH radical were conducted in the

same conditions using CHEMKIN-PRO [56]. These analyses evaluate how A-factor of each reaction in the kinetic model of this study influences the formation of OH radicals. The results are given as sensitivity coefficients of reactions. A positive coefficient means the relevant reaction having a promoting effect on the production of OH radical. On the other hand, a negative coefficient indicates the inhibiting effect of the relevant reaction on the production of OH radical. The result of the sensitivity analyses at the moment 75% decomposition of EHN is presented in Figure 11. It is found that the reaction of EHN decomposition presents a high promoting effect on the production of OH radicals in the early stage of combustion at all examined  $T_c$ . This reaction becomes less sensitive at the time of the total decomposition of EHN. There is no other reaction of nitrogen chemistry being sensitive to the formation of OH radical.

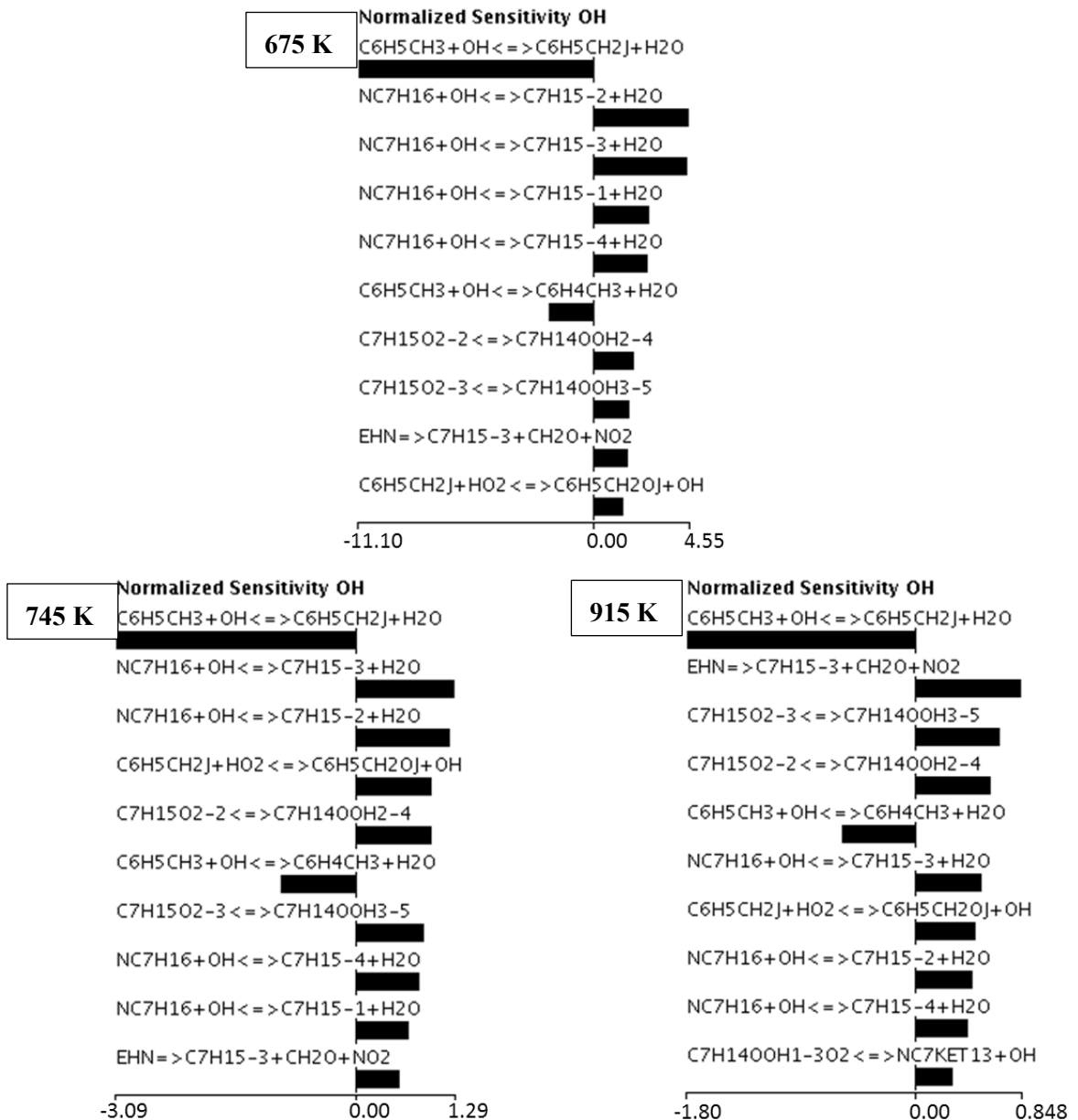


**Figure 11.** Results of sensitivity analyses on the formation of OH radical at the moment 75% decomposition of EHN at three different  $T_c$ : 675 K, 745 K, and 915 K for EHN doping level of 0.1% mol. at  $P_c = 10$  bar and  $\Phi = 1$ .

## 5. Conclusions

Experiments and modeling works are performed to investigate the EHN promoting effect on LTC-relevant conditions. The IDT of the neat and doped fuels were measured in a RCM at  $\Phi = 1$ ,  $P_c = 10$  bar and  $T_c = 675 - 960$  K. The neat fuel is a low-octane gasoline fuel (RON = 84) containing toluene and *n*-heptane. The doping level of EHN varies from 0.1 to 1% molar basis.

At the experimental conditions (10 bar,  $\Phi = 1$ ), it is observed that EHN provides a promoting effect on the surrogate reactivity at all examined  $T_c$  (675 – 960 K). This effect increases with EHN doping levels. The NTC behavior of the surrogate fuel is mitigated by the addition of EHN and at doping level of 1% mol., EHN suppresses the NTC region. This feature was not observed through our previous study on EHN effect at lean condition [19]. The EHN promoting effect is found to be lowest at  $T_c$  near 740 K and then increases with  $T_c$ .

The heat releases during the compression process are observed in RCM tests of the doped fuels because of the rapid decomposition of EHN at  $T_c > 750$  K. This implies the measured EHN promoting effect in a RCM at this  $T_c$  range depends partly on the compression time of the considered machine. Additionally, the chemical activity of fuel gas mixture during the compression process have to be carefully considered to get reliable simulation results.

Kinetic modeling shows a good coherence with experiments. The model reproduces properly the EHN promoting effect over the whole range of investigated  $T_c$  and doping levels. EHN decompositions during the compression process are reasonably simulated, which is validated by the pressure histories simulations. By applying the same kinetic model and the same RCM simulation method, a better agreement between simulations and experiments was observed while simulating the EHN effect at lean condition from our previous work [19]. It was found that EHN was less effective at low  $T_c$  ( $< 800$  K) at lean condition than at stoichiometric condition due to its slower decomposition.

The validation of the kinetic model by literature data was conducted. The results indicate that this

kinetic model is capable of simulate reliably EHN promoting effect on different fuels at LTC-relevant conditions.

Goldsborough et al. [18] indicated that EHN effect was linked to the formation of OH radicals by the two reactions:  $\text{NO} + \text{HO}_2 = \text{NO}_2 + \text{OH}$  and  $\text{NO}_2 + \text{H} = \text{NO} + \text{OH}$ . The reactions of hydrocarbon radicals and peroxy radicals with  $\text{NO}_x$  such as  $\text{R} + \text{NO}_2 = \text{RO} + \text{NO}$  and  $\text{RO}_2 + \text{NO} = \text{RO} + \text{NO}_2$  could compete with the above reactions and then reduce the effect of EHN. The observation of Goldsborough et al. is quite different to the result of this study. Numerical analyses of this study indicate that EHN effect is due to the OH radical formation and  $\text{NO}_2\text{-NO}$  loop. In the presence of EHN, a supplementary source of OH radicals is formed by the reactions of  $\text{C}_7\text{H}_{15}\text{-3}$  radical and from the reaction  $\text{NO} + \text{HO}_2 = \text{NO}_2 + \text{OH}$  in the  $\text{NO}_2\text{-NO}$  loop.  $\text{NO}_2$  generated from EHN decomposition can react with benzyl radical ( $\text{C}_6\text{H}_5\text{CH}_2$ ) to form  $\text{C}_6\text{H}_5\text{CH}_2\text{O}$  radical and NO. These two factors enhance the initiation and propagation steps of the fuel oxidation. The reactions between NO and *n*-heptyl peroxy radicals are found to be the main cause of EHN effect on NTC region of the surrogate fuel oxidation. It is also found that the formation of nitroethane ( $\text{C}_2\text{H}_5\text{NO}_2$ ) is the main reason, why EHN promoting effect is minimum at  $T_c$  around 740 K.

This study contributes to the fundamental understanding of nitrogen-based cetane booster additive on fuel reactivity. The validated kinetic model can help to investigate EHN promoting effect in different internal combustion engines using multiple fuels chemistries.

## References

- [1] A.K. Agarwal, A.P. Singh, R.K. Maurya, Evolution, challenges and path forward for low

- temperature combustion engines, *Progress in Energy and Combustion Science* 61 (2017) 1–56.
- [2] T.K. Sharma, G.A.P. Rao, K.M. Murthy, Homogeneous Charge Compression Ignition (HCCI) Engines: A Review, *Archives of Computational Methods in Engineering* 23 (2016) 623–657.
  - [3] G. Kalghatgi, B. Johansson, Gasoline compression ignition approach to efficient, clean and affordable future engines, *Proceedings of the Institution of Mechanical Engineers, Part D: Journal of Automobile Engineering* 232 (2017) 118–138.
  - [4] R.D. Reitz, G. Duraisamy, Review of high efficiency and clean reactivity controlled compression ignition (RCCI) combustion in internal combustion engines, *Progress in Energy and Combustion Science* 46 (2015) 12–71.
  - [5] L. Manofsky, J. Vavra, D.N. Assanis, A. Babajimopoulos, Bridging the Gap between HCCI and SI: Spark-Assisted Compression Ignition, *SAE Technical Paper* 2011-01-1179 (2011).
  - [6] R.K. Hanson, D.F. Davidson, Recent advances in laser absorption and shock tube methods for studies of combustion chemistry, *Progress in Energy and Combustion Science* 44 (2014) 103–114.
  - [7] S.S. Goldsborough, S. Hochgreb, G. Vanhove, M.S. Wooldridge, H.J. Curran, C.-J. Sung, Advances in rapid compression machine studies of low- and intermediate-temperature autoignition phenomena, *Progress in Energy and Combustion Science* 63 (2017) 1–78.
  - [8] C. Mohamed, Suppression of reaction during rapid compression and its effect on ignition delay, *Combustion and Flame* 112 (1998) 438–444.
  - [9] H.J. Curran, P. Gaffuri, W.J. Pitz, C.K. Westbrook, A Comprehensive Modeling Study of n-Heptane Oxidation, *Combustion and Flame* 114 (1998) 149–177.
  - [10] D. Seyferth, The Rise and Fall of Tetraethyllead. 2, *Organometallics* 22 (2003) 5154–5178.
  - [11] W.E. Robbins, R.R. Audette, N.E. Reynolds, Performance and Stability of Some Diesel Fuel Ignition Quality Improvers, *SAE Technical Paper* 510200 (1951).
  - [12] A.B. Rode, K. Chung, Y.-W. Kim, I.S. Hong, Synthesis and Cetane-Improving Performance of 1,2,4,5-Tetraoxane and 1,2,4,5,7,8-Hexaoxonane Derivatives, *Energy Fuels* 24 (2010) 1636–1639.
  - [13] Y.R. Luo, *Handbook of Bond Dissociation Energies in Organic Compounds*, CRC Press (2002).
  - [14] J. Kaddatz, M. Andrie, R.D. Reitz, S. Kokjohn, Light-Duty Reactivity Controlled Compression Ignition Combustion Using a Cetane Improver, *SAE Technical Paper* 2012-01-1110 (2012).
  - [15] A.B. Dempsey, N.R. Walker, R.D. Reitz, Effect of Cetane Improvers on Gasoline, Ethanol, and Methanol Reactivity and the Implications for RCCI Combustion, *SAE Int. J. Fuels Lubr.* 6 (2013) 170–187.
  - [16] M. Hartmann, K. Tian, C. Hofrath, M. Fikri, A. Schubert, R. Schießl, R. Starke, B. Atakan, C. Schulz, U. Maas, F. Kleine Jäger, K. Kühling, Experiments and modeling of ignition delay times, flame structure and intermediate species of EHN-doped stoichiometric n-heptane/air combustion, *Proc. Combust. Inst.* 32 (2009) 197–204.

- [17] P. Cadman, Shock tube combustion of liquid hydrocarbon sprays of toluene, *Phys. Chem. Chem. Phys.* 3 (2001) 4301–4309.
- [18] S.S. Goldsborough, M.V. Johnson, C. Banyon, W.J. Pitz, M.J. McNenly, Experimental and modeling study of fuel interactions with an alkyl nitrate cetane enhancer, 2-ethyl-hexyl nitrate, *Proc. Combust. Inst.* 35 (2015) 571–579.
- [19] M. D. Le, M. Matrat, A. Ben Amara, F. Foucher, B. Moreau, Y. Yu, P-A. Glaude, Exploring and Modeling the Chemical Effect of a Cetane Booster Additive in a Low-Octane Gasoline Fuel, *SAE Technical Paper* 2019-24-0069 (2019).
- [20] N. Bourgeois, S.S. Goldsborough, G. Vanhove, M. Duponcheel, H. Jeanmart, F. Contino, CFD simulations of Rapid Compression Machines using detailed chemistry, *Proceedings of the Combustion Institute* 36 (2017) 383–391.
- [21] L. Yu, Z. Wu, Y. Qiu, Y. Qian, Y. Mao, X. Lu, Ignition delay times of decalin over low-to-intermediate temperature ranges, *Combustion and Flame* 196 (2018) 160–173.
- [22] K. Alexandrino, M.U. Alzueta, H.J. Curran, An experimental and modeling study of the ignition of dimethyl carbonate in shock tubes and rapid compression machine, *Combustion and Flame* 188 (2018) 212–226.
- [23] M. Wang, K. Zhang, G. Kukkadapu, S.W. Wagnon, M. Mehl, W.J. Pitz, C.-J. Sung, Autoignition of trans -decalin, a diesel surrogate compound, *Combustion and Flame* 194 (2018) 152–163.
- [24] M. Pochet, V. Dias, B. Moreau, F. Foucher, H. Jeanmart, F. Contino, Experimental and numerical study, under LTC conditions, of ammonia ignition delay with and without hydrogen addition, *Proc. Combust. Inst.* 37 (2019) 621–629.
- [25] J. Herzler, M. Fikri, K. Hitzbleck, R. Starke, C. Schulz, P. Roth, G.T. Kalghatgi, Shock-tube study of the autoignition of n-heptane/toluene/air mixtures at intermediate temperatures and high pressures, *Combustion and Flame* 149 (2007) 25–31.
- [26] M. Mehl, W.J. Pitz, C.K. Westbrook, H.J. Curran, Kinetic modeling of gasoline surrogate components and mixtures under engine conditions, *Proc. Combust. Inst.* 33 (2011) 193–200.
- [27] W. Yuan, Y. Li, P. Dagaut, J. Yang, F. Qi, Investigation on the pyrolysis and oxidation of toluene over a wide range conditions. II. A comprehensive kinetic modeling study, *Combustion and Flame* 162 (2015) 22–40.
- [28] M. Keita, A. Nicolle, A.E. Bakali, A wide range kinetic modeling study of PAH formation from liquid transportation fuels combustion, *Combustion and Flame* 174 (2016) 50–67.
- [29] G.R. Galimova, V.N. Azyazov, A.M. Mebel, Reaction mechanism, rate constants, and product yields for the oxidation of Cyclopentadienyl and embedded five-member ring radicals with hydroxyl, *Combustion and Flame* 187 (2018) 147–164.
- [30] A.R. Ghildina, A.D. Oleinikov, V.N. Azyazov, A.M. Mebel, Reaction mechanism, rate constants, and product yields for unimolecular and H-assisted decomposition of 2,4-cyclopentadienone and oxidation of cyclopentadienyl with atomic oxygen, *Combustion and*

Flame 183 (2017) 181–193.

- [31] A.D. Oleinikov, V.N. Azyazov, A.M. Mebel, Oxidation of cyclopentadienyl radical with molecular oxygen, Combustion and Flame 191 (2018) 309–319.
- [32] H. Bornemann, F. Scheidt, W. Sander, Thermal decomposition of 2-ethylhexyl nitrate (2-EHN), Int. J. Chem. Kinet. 34 (2002) 34–38.
- [33] J. Morin, Y. Bedjanian, Thermal decomposition of n-propyl and n-butyl nitrates, Journal of Analytical and Applied Pyrolysis 124 (2017) 576–583.
- [34] H.O. Pritchard, Thermal decomposition of isoctyl nitrate, Combustion and Flame 75 (1989) 415–416.
- [35] P. Glarborg, J.A. Miller, B. Ruscic, S.J. Klippenstein, Modeling nitrogen chemistry in combustion, Progress in Energy and Combustion Science 67 (2018) 31–68.
- [36] M.E. Fuller, C.F. Goldsmith, On the relative importance of HONO versus HNO<sub>2</sub> in low-temperature combustion, Proceedings of the Combustion Institute 37 (2018) 695–702.
- [37] K. Zhang, P. Glarborg, X. Zhou, L. Zhang, L. Ye, G. Dayma, Experimental and Kinetic Modeling Study of Nitroethane Pyrolysis at a Low Pressure, Energy Fuels 30 (2016) 7738–7745.
- [38] J.M. Anderlohr, R. Bounaceur, A. Pires Da Cruz, F. Battin-Leclerc, Modeling of autoignition and NO sensitization for the oxidation of IC engine surrogate fuels, Combustion and Flame 156 (2009) 505–521.
- [39] H. Zhao, L. Wu, C. Patrick, Z. Zhang, Y. Rezgui, X. Yang, G. Wysocki, Y. Ju, Studies of low temperature oxidation of n-pentane with nitric oxide addition in a jet stirred reactor, Combustion and Flame 197 (2018) 78–87.
- [40] Z. Chen, P. Zhang, Y. Yang, M.J. Brear, X. He, Z. Wang, Impact of nitric oxide (NO) on n-heptane autoignition in a rapid compression machine, Combustion and Flame 186 (2017) 94–104.
- [41] P.-A. Glaude, N. Marinov, Y. Koshiishi, N. Matsunaga, M. Hori, Kinetic Modeling of the Mutual Oxidation of NO and Larger Alkanes at Low Temperature, Energy Fuels 19 (2005) 1839–1849.
- [42] C.L. Rasmussen, A.E. Rasmussen, P. Glarborg, Sensitizing effects of NO<sub>x</sub> on CH<sub>4</sub> oxidation at high pressure, Combustion and Flame 154 (2008) 529–545.
- [43] P. Dagaut, F. Lecomte, S. Chevailler, M. Cathonnet, Mutual Sensitization of the Oxidation of Nitric Oxide and Simple Fuels Over an Extended Temperature Range, Combustion Science and Technology 148 (1999) 27–57.
- [44] C.J. Howard, Kinetic Study of the Equilibrium HO<sub>2</sub> + NO = OH + NO<sub>2</sub> and the Thermochemistry of HO<sub>2</sub>, J. Am. Chem. Soc. 102 (1980) 6937–6941.
- [45] M.W. Bardwell, A. Bacak, M. Teresa Raventos, C.J. Percival, G. Sanchez-Reyna, D.E. Shallcross, Kinetics of the HO<sub>2</sub> + NO reaction, Phys. Chem. Chem. Phys. 5 (2003) 2381–2385.

- [46] C. Chen, B.C. Shepler, B.J. Braams, J.M. Bowman, Quasiclassical trajectory calculations of the HO<sub>2</sub> + NO reaction on a global potential energy surface, *Phys. Chem. Chem. Phys.* 11 (2009) 4722–4727.
- [47] A. Bacak, M.W. Bardwell, M.T. Raventos, C.J. Percival, G. Sanchez-Reyna, D.E. Shallcross, Kinetics of the Reaction of CH<sub>3</sub>O<sub>2</sub> + NO, *J. Phys. Chem. A* 108 (2004) 10681–10687.
- [48] N. Butkovskaya, A. Kukui, G. Le Bras, Pressure and temperature dependence of methyl nitrate formation in the CH<sub>3</sub>O<sub>2</sub> + NO reaction, *The journal of physical chemistry. A* 116 (2012) 5972–5980.
- [49] A. Lesar, M. Hodoscek, E. Drougas, A.M. Kosmas, Quantum mechanical investigation of the atmospheric reaction CH<sub>3</sub>O<sub>2</sub> + NO, *J. Phys. Chem. A* 110 (2006) 7898–7903.
- [50] M.M. Maricq, J.J. Szente, Kinetics of the Reaction between Ethylperoxy Radicals and Nitric Oxide, *J. Phys. Chem.* 100 (1996) 12374–12379.
- [51] D.L. Ranschaert, N.J. Schneider, M.J. Elrod, Kinetics of the C<sub>2</sub>H<sub>5</sub>O<sub>2</sub> + NO<sub>x</sub> Reactions, *J. Phys. Chem. A* 104 (2000) 5758–5765.
- [52] R. Atkinson, D.L. Baulch, R.A. Cox, R.F. Hampson, J.A. Kerr, J. Troe, *J. Phys. Chem. Ref. Data* 21 (1992) 1125.
- [53] Z.F. Xu, M.C. Lin, Kinetics and mechanism for the CH<sub>2</sub>O + NO<sub>2</sub> reaction, *Int. J. Chem. Kinet.* 35 (2003) 184–190.
- [54] G. Moréac, P. Dagaut, J.F. Roesler, M. Cathonnet, Nitric oxide interactions with hydrocarbon oxidation in a jet-stirred reactor at 10 atm, *Combustion and Flame* 145 (2006) 512–520.
- [55] S. Tanaka, F. Ayala, J.C. Keck, A reduced chemical kinetic model for HCCI combustion of primary reference fuels in a rapid compression machine, *Combustion and Flame* 133 (2003) 467–481.
- [56] Reaction Design, CHEMKIN-PRO, San Diego, 2017.
- [57] M. Hartmann, I. Gushterova, M. Fikri, C. Schulz, R. Schießl, U. Maas, Auto-ignition of toluene-doped n-heptane and iso-octane/air mixtures, *Combustion and Flame* 158 (2011) 172–178.
- [58] J. Zhang, V. Burklé-Vitzthum, P.-M. Marquaire, NO<sub>2</sub>-promoted oxidation of methane to formaldehyde at very short residence time. Part I, *Chemical Engineering Journal* 189-190 (2012) 393–403.
- [59] A. Dubreuil, F. Foucher, C. Mounaïm-Rousselle, G. Dayma, P. Dagaut, HCCI combustion, *Proceedings of the Combustion Institute* 31 (2007) 2879–2886.
- [60] K. Glänzer, J. Troe, Thermische Zerfallsreaktionen von Nitroverbindungen I, *HCA* 55 (1972) 2884–2893.
- [61] O. Mathieu, B. Giri, A.R. Agard, T.N. Adams, J.D. Mertens, E.L. Petersen, Nitromethane ignition behind reflected shock waves, *Fuel* 182 (2016) 597–612.
- [62] Y.-X. Zhang, S.H. Bauer, Gas-Phase Pyrolyses of 2-Nitropropane and 2-Nitropropanol, *J. Phys. Chem. A* 104 (2000) 1207–1216.

- [63] F. Battin-Leclerc, Detailed chemical kinetic models for the low-temperature combustion of hydrocarbons with application to gasoline and diesel fuel surrogates, *Progress in Energy and Combustion Science* 34 (2008) 440–498.
- [64] W. Yuan, Y. Li, P. Dagaut, J. Yang, F. Qi, Investigation on the pyrolysis and oxidation of toluene over a wide range conditions. I. Flow reactor pyrolysis and jet stirred reactor oxidation, *Combustion and Flame* 162 (2015) 3–21.
- [65] G. da Silva, J.W. Bozzelli, Benzoxy radical decomposition kinetics, *The journal of physical chemistry. A* 113 (2009) 6979–6986.
- [66] R. Bounaceur, I. Da Costa, R. Fournet, F. Billaud, F. Battin-Leclerc, Experimental and modeling study of the oxidation of toluene, *Int. J. Chem. Kinet.* 37 (2005) 25–49.